



Evidence that solar wind fluctuations substantially affect global convection and substorm occurrence

L. R. Lyons,¹ H.-J. Kim,¹ X. Xing,¹ S. Zou,¹ D.-Y. Lee,² C. Heinselman,³ M. J. Nicolls,³ V. Angelopoulos,⁴ D. Larson,⁵ J. McFadden,⁵ A. Runov,⁵ and K.-H. Fornacon⁶

Received 23 March 2009; revised 17 June 2009; accepted 5 August 2009; published 10 November 2009.

[1] We have used examples of Poker Flat and Sondrestrom incoherent-scatter radar observations of flows within the ionospheric mapping of the nightside plasma sheet and of Time History of Events and Macroscale Interactions during Substorms (THEMIS) spacecraft observations within the nightside plasma sheet to investigate whether the features found in the companion paper by Kim *et al.* (2009) within the dayside polar cap are also seen within the nightside plasma sheet. We find evidence that this is indeed the case: intensified interplanetary ULF fluctuations substantially enhance nightside convection flows and the fluctuations are reflected in the fluctuation power of the nightside flows. Additionally, our observations show evidence for an enhancement of earthward convection within the inner plasma sheet and an increase in plasma pressure within the plasma sheet in association with enhanced interplanetary ULF fluctuations. We have also found evidence that the enhancement in convection and plasma sheet pressure associated with strong interplanetary fluctuations may lead to a dramatic increase in substorm occurrence under northward interplanetary magnetic field conditions. More detailed testing of the above results is needed. However, if corroborated, it would indicate that interplanetary ULF fluctuations have a substantial effect on global convection and are an important contributor to the large-scale transfer of solar wind energy to the magnetosphere-ionosphere system, to plasma sheet structure and dynamics, and to the occurrence of disturbances such as substorms.

Citation: Lyons, L. R., *et al.* (2009), Evidence that solar wind fluctuations substantially affect global convection and substorm occurrence, *J. Geophys. Res.*, 114, A11306, doi:10.1029/2009JA014281.

1. Introduction

[2] In the companion paper by Kim *et al.* [2009], we examined the relation of the strength of dayside convection with solar wind conditions using Sondrestrom incoherent scatter radar (ISR) observations of high-latitude ionospheric flows. We found evidence that, in addition to the well-known effects of the interplanetary magnetic field (IMF) direction and magnitude and the solar wind dynamic pressure, which are clearly seen in radar observations [e.g., Boudouridis *et al.*, 2007; Zou *et al.*, 2008], ULF fluctuations in the solar wind

are a potentially important driver of ionospheric convection within the dayside polar cap. We also found evidence that enhanced ULF fluctuations within the solar wind lead to enhanced ULF fluctuations of the dayside ionospheric flow. We argued that this implies that solar wind ULF power may be an important contributor to the strength of coupling of solar wind energy to the magnetosphere-ionosphere system, and we speculated that resonance between the solar wind fluctuations and natural magnetospheric oscillation frequencies might be responsible for the connection between ionospheric convection and solar wind ULF power. The high correlations between ULF power in the solar wind dynamic pressure P_{dyn} and the IMF makes it difficult to determine which parameter is the driver of the convection enhancements. However, individual examples were used to indicate that IMF fluctuations affect convection independently of effects from P_{dyn} fluctuations, and Kim *et al.* [2009] suggested that IMF and P_{dyn} fluctuations may work together to enhance the convection more than would fluctuations in only the IMF or P_{dyn} .

[3] Here we investigate whether ULF fluctuations within the solar wind also substantially affect the strength and ULF fluctuations of nightside convection flows, which would suggest that solar wind fluctuations drive a global response of the magnetosphere-ionosphere system. We use ionospheric observations from the Sondrestrom ISR and the Poker Flat

¹Department of Atmospheric and Oceanic Sciences, University of California, Los Angeles, California, USA.

²Department of Astronomy and Space Science, Chungbuk National University, Cheongju, South Korea.

³Center for Geospace Studies, SRI International, Menlo Park, California, USA.

⁴Department of Earth and Space Sciences, Institute for Geophysics and Planetary Physics, University of California, Los Angeles, California, USA.

⁵Space Sciences Laboratory, University of California, Berkeley, California, USA.

⁶Institut für Geophysik und Extraterrestrische Physik, Technische Universität Braunschweig, Braunschweig, Germany.

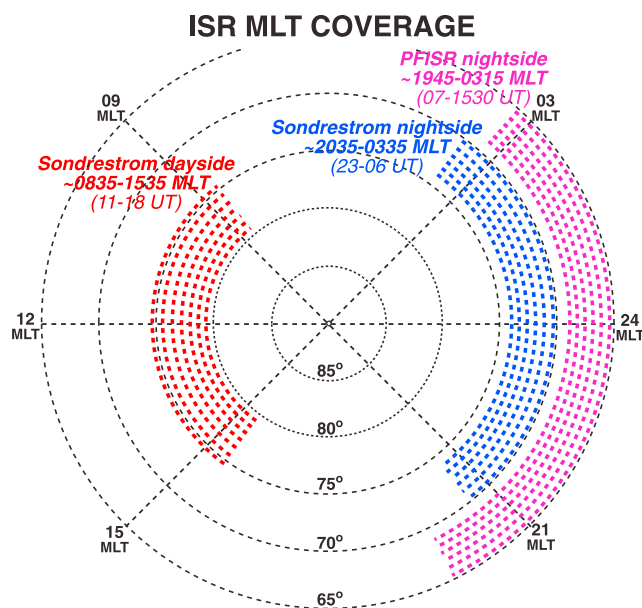


Figure 1. Latitudinal and magnetic local time (MLT) coverage of the radars used in this study.

ISR (PFISR) within the poleward and equatorward portions of the ionospheric mapping of the plasma sheet, respectively. We also use in situ Time History of Events and Macroscale Interactions during Substorms (THEMIS) multispacecraft observations within the nightside plasma sheet to investigate flows within the plasma sheet itself, and, together with observations of substorm occurrence from the THEMIS ground all-sky imagers, to investigate the effect of the solar wind ULF fluctuations on substorm occurrence.

[4] We do not yet have a sufficient number of nightside radar runs and THEMIS orbits to do a detailed statistical analysis as done with the dayside radar observations by *Kim et al.* [2009]. Instead we show comparisons between observations during individual radar runs and THEMIS orbits under different conditions. For these comparisons, we select runs/orbits that had prolonged periods of the same type of solar wind condition, specifically prolonged periods of steady northward or steady southward IMF and prolonged periods of interplanetary ULF fluctuations. We take advantage of the fact that, during some periods, the IMF stays predominantly northward while having strong ULF fluctuations, which gives very distinctive comparisons with observations during periods of steady northward IMF. We also make comparisons between runs/orbits with steady southward IMF and strongly fluctuating IMF that includes periods of southward IMF. These comparisons will be shown to give evidence that solar wind ULF fluctuations have a substantial effect on global convection and plasma sheet dynamics.

2. Observational Approach

[5] Both of the radars were operated in modes selected to maximize latitudinal coverage and temporal resolution of flow measurements. Nightside runs were ~ 7 – 8 h in length centered approximately at magnetic midnight. The coverage of the radars in latitude and magnetic local time (MLT) is illustrated in Figure 1. The mode selected for the nightside

Sondrestrom ISR radar runs is identical to that for the dayside radar runs used in the work of *Zou et al.* [2008] and *Kim et al.* [2009], except that the radar looked equatorward rather than poleward. This gives flow measurements versus invariant latitude Λ along the portion of the radar magnetic meridian equatorward, rather than poleward, of the radar location ($\Lambda = 74^\circ$). Thus, while the dayside measurements extend poleward from near the expected location of the polar cap boundary into the polar cap, the nightside measurements extend equatorward from near the expected location of the polar cap into the poleward portion of the ionospheric mapping of the plasma sheet. Observations from 25 nightside runs from December 2007 through April 2008 were available for this study. PFISR is located at $\Lambda = 65.4^\circ$ near Fairbanks, Alaska. The operation mode for the nightside runs of PFISR used here is described in the work of *Zou et al.* [2009] and *Lyons et al.* [2009], and flow measurements along the radar magnetic meridian extend poleward from the radar location to near the equatorward boundary of the Sondrestrom radar field-of-view. Observations from 88 nightside runs from March 2007 through May 2008 were available for this study.

[6] The THEMIS mission consists of five spacecraft orbiting near the equatorial plane. Plasma moments are used here that are obtained from the Electrostatic Analyzer (ESA) and Solid State Telescope (SST), which cover the particle energy range 5 eV to 6 MeV for ions and 5 eV to 1 MeV for electrons [*Angelopoulos, 2008; McFadden et al., 2008*]. Magnetic field data are from the Fluxgate Magnetometer [*Auster et al., 2008*]. We use observations from the first THEMIS tail season from February to mid-March 2008, when the spacecraft apogees were near to slightly duskward of magnetic midnight.

3. Observation Examples

[7] We first show observations from four of our dayside Sondrestrom runs, which we use to illustrate the results found by *Kim et al.* [2009] and for comparison with what is seen on the nightside. We then present and discuss examples of the nightside radar observations followed by examples of THEMIS spacecraft observations. We use the IMF to indicate periods with and without interplanetary pulsations.

3.1. Radar Flow Observations

[8] Figure 2 shows observations from four of our dayside Sondrestrom runs. Both the east–west and north–south components of flow speeds are plotted at four magnetic latitudes from 75° to 78° , along with the solar wind speed and IMF B_y and B_z as time shifted to the magnetopause nose by the Weimer technique [*Weimer et al., 2002*]. Dashed horizontal lines are labeled with the measurement latitude and represent zero velocity, values being positive for northward and for eastward velocities. These examples illustrate the substantial enhancement of flow speeds and of flow fluctuations that occur when the IMF has large-amplitude ULF Alfvénic fluctuations (Figure 2, right) relative to when the IMF is steady (Figure 2, left). Figure 2 compares (Figure 2, top) the observations during runs that occurred under predominantly northward IMF conditions with (Figure 2, bottom) the observations from a run with a prolonged period of steady southward IMF with those from

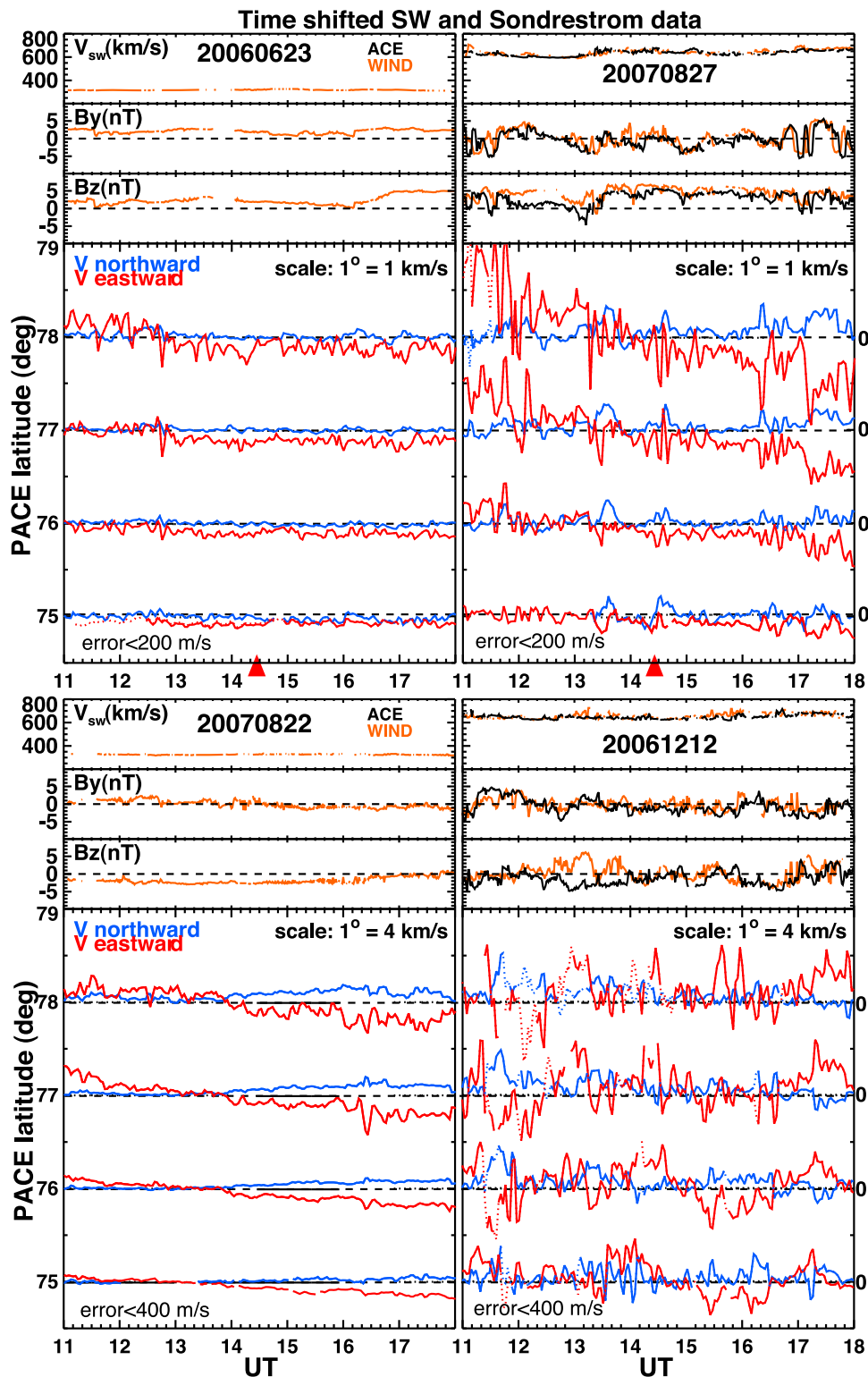


Figure 2. Observations of east/west and north/south components of flow speeds at four magnetic latitudes from 75° to 78°, along with the solar wind speed and IMF B_y and B_z as time shifted to the magnetopause nose by the Weimer technique, from four of our dayside Sondrestrom runs. Dashed horizontal lines are labeled with the measurement latitude and represent zero velocity, values being positive for northward and for eastward velocities.

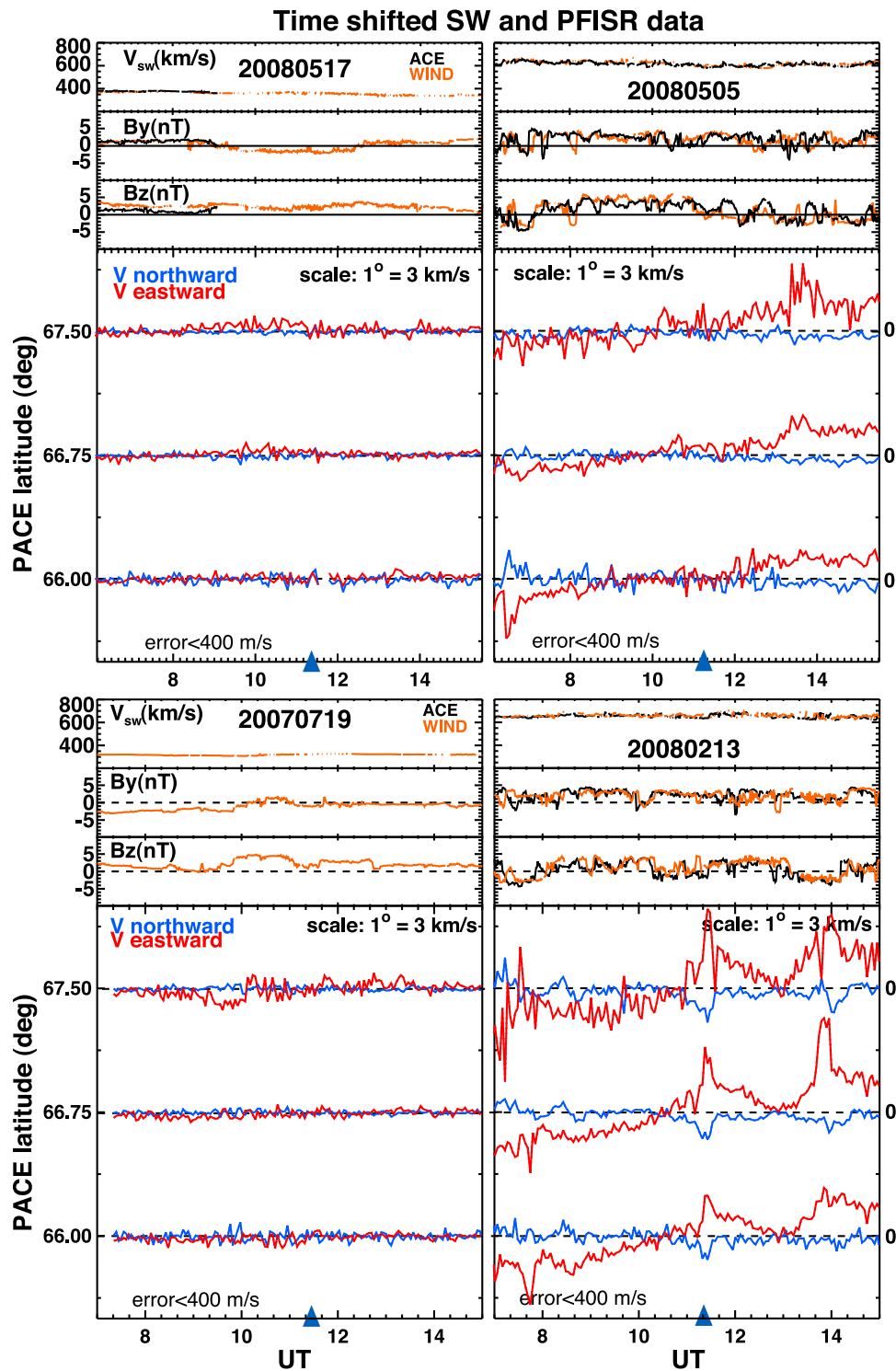


Figure 3. Same as Figure 2 except for four of our nightside PFISR runs. Flows are shown at three latitudes from 66° to 67.5° .

a run with north–south fluctuating IMF during a high-speed stream. Note that the flow speed scale in Figure 2 (top; northward IMF) is expanded by a factor of four relative to the scale in Figure 2 (bottom).

[9] Figure 3 (left) shows observations from PFISR runs that have been selected to have predominantly steady northward IMF and to have predominantly northward IMF with

large amplitude Alfvénic fluctuations. It was not possible to find an example with large-amplitude Alfvénic fluctuations for which the IMF stayed northward for the entire run, but the IMF stayed almost entirely northward from ~ 0700 to 1200 UT during the 5 May 2008 run (Figure 3, top) and from 0745 to 1015 UT and from 1120 to 1310 UT during the 13 February 2008 run (Figure 3, bottom). The flow response to the fluctuating IMF relative to that for steady northward

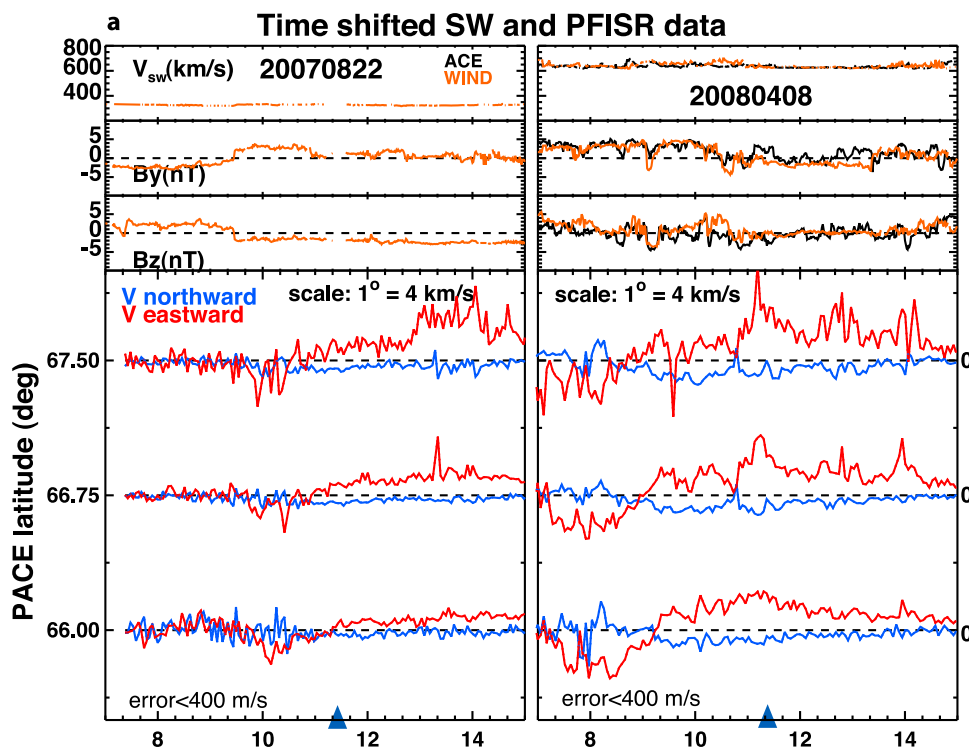


Figure 4. Same as Figure 2, except for six of our nightside PFISR runs. Flows are shown at three latitudes from 66° to 67.5° .

IMF can be seen to be very similar within the ionospheric mapping of the inner plasma sheet to what is seen in the Sondrestrom observations within the dayside polar cap in Figure 2 (top). The increase in flow speed is particularly clearly seen in the east–west flows, but a small difference can also be seen in the north–south flows. An enhancement in the level of fluctuation can be clearly seen as well.

[10] The V_{sw} , B_y , and B_z plots in Figure 4 compare PFISR observations during two runs with prolonged periods of relatively steady, moderately southward IMF (Figure 4, left) to observations during two runs with north–south fluctuating IMF (Figure 4, right), the largest magnitudes of the southward excursions of the IMF being about the same as the magnitudes of the steady southward IMF during the runs (Figure 4, left). It can be seen that the magnitudes of the east–west flows are about the same, or perhaps a little stronger, during the fluctuating IMF runs as during the steady southward IMF, despite the IMF being southward for shorter overall time periods. What is particularly interesting here is that the equatorward directed flows are substantially larger for the fluctuating IMF cases, which is an indication of stronger earthward convection of plasma sheet particles within the inner plasma sheet. Such enhanced convection could be associated with a reduction in shielding, since shielding reduces earthward convection near and earthward of the equatorward boundary of the plasma sheet.

[11] The V plots in Figure 4 compare a run with relatively steady, strongly southward IMF after 1000 UT (14 July 2007) to a run with fluctuating IMF (5 March 2008) that mostly remains southward, but for which southward field magnitudes mostly remain less than those on 14 July 2007. It can be seen that, despite the weaker southward IMF, the flow speeds on 5 March 2008 have about the same magnitudes as do those

after 1000 UT on 14 July 2007. Note also that the 5 March 2008 run was during a slow solar wind stream, consistent with the result of *Kim et al.* [2009] that the effect of IMF fluctuations on the flows is independent of any direct effect of the solar wind speed. It is also interesting that, while equatorward convection is seen during the strong southward IMF period on 14 July 2007, equatorward convection is of about the same strength during the three runs with fluctuating IMF runs, despite the weaker and less persistent southward IMF.

[12] The above examples of PFISR observations show that most aspects of the convection response to fluctuating IMF that are seen within the dayside polar cap are also seen within the equatorward portion of the nightside plasma sheet. In particular, we see evidence for a substantial enhancement of earthward convection within the inner plasma sheet. An enhancement in the fluctuation level of convection flows during fluctuating IMF conditions is not as clear for the examples in Figure 4 as for the northward IMF examples in Figure 3, but evidence for such an enhancement is discussed later.

[13] Figure 5 shows observations from nightside Sondrestrom radar runs that have been selected to have predominantly steady northward IMF (Figure 5, left) and to have northward IMF with large amplitude Alfvénic fluctuations (Figure 5, right; the 13 February 2008 example has predominantly northward IMF throughout and the 19 February 2008 example has predominantly northward IMF before 0215 UT followed by very slightly negative B_z). The observations show that, for steady northward IMF conditions, there are substantially higher fluctuating flows within the poleward portion of the plasma sheet than are seen within the dayside polar cap (see Figure 2, left) and the more equatorward portion of the plasma sheet (see Figure 3, left), which may

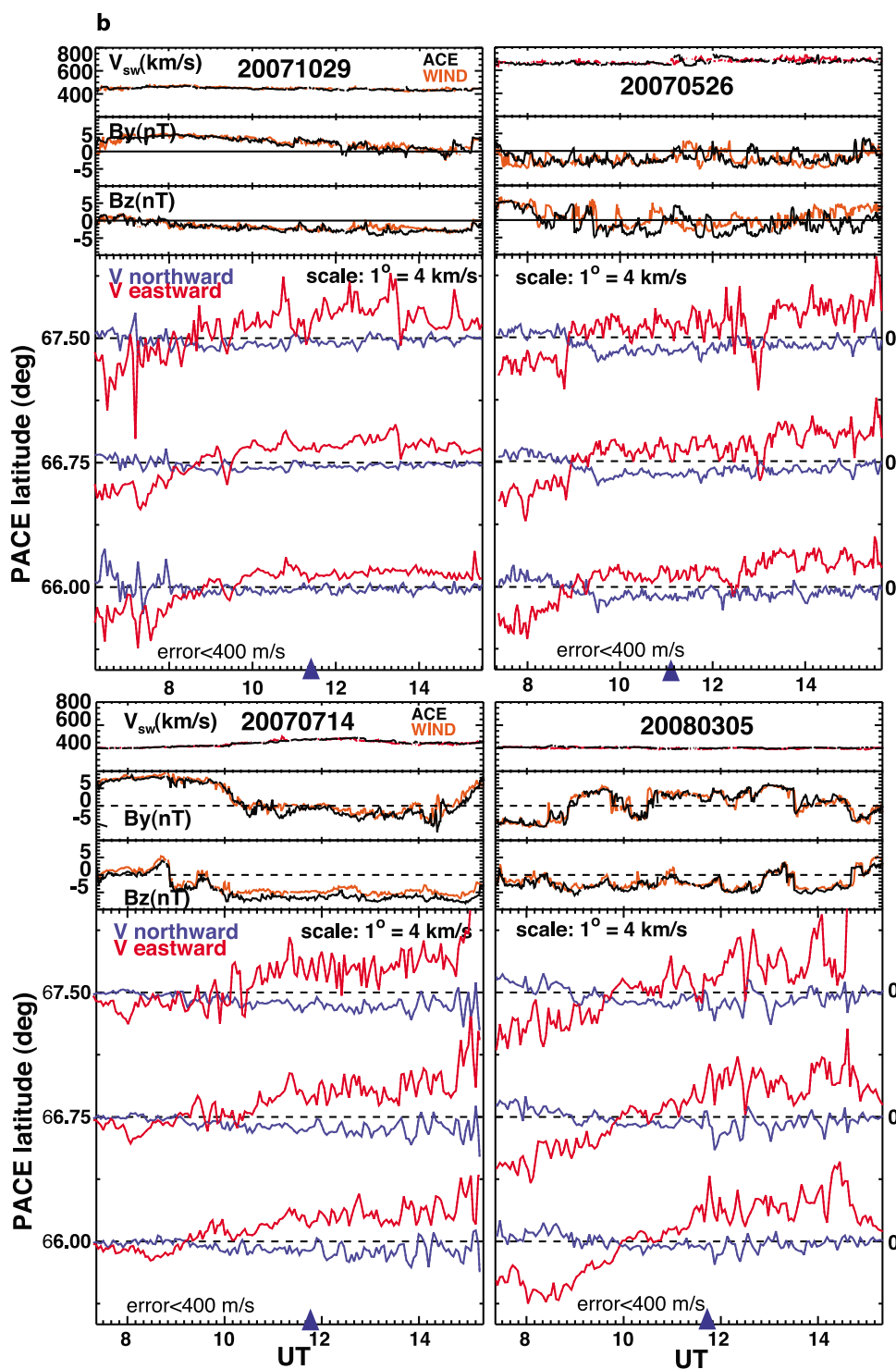


Figure 4. (continued)

well be associated with polar boundary auroral intensifications (PBIs). While PBIs are stronger and more frequent during disturbed conditions, PBIs are common in this region during quiet times. They are known to be associated with flow enhancements, which have been seen both in the ionosphere [*de la Beaujardière et al.*, 1994] and in situ within the tail plasma sheet [*Lyons et al.*, 1999; *Zesta et al.*, 2000, 2006].

[14] Comparing the flows in Figure 5 shows some evidence for larger flows and larger flow fluctuations during the

runs with large-amplitude Alfvénic fluctuations, but the distinction is not as clear as seen within the dayside polar cap and the more equatorward portion of the plasma sheet. It is fairly clear, however, that the north–south velocities are roughly equally distributed about zero for the steady IMF runs. However, there is a predominance of equatorward directed flows during the fluctuating IMF runs, which can be seen quite clearly for the 13 February 2008 example having predominantly northward IMF throughout.

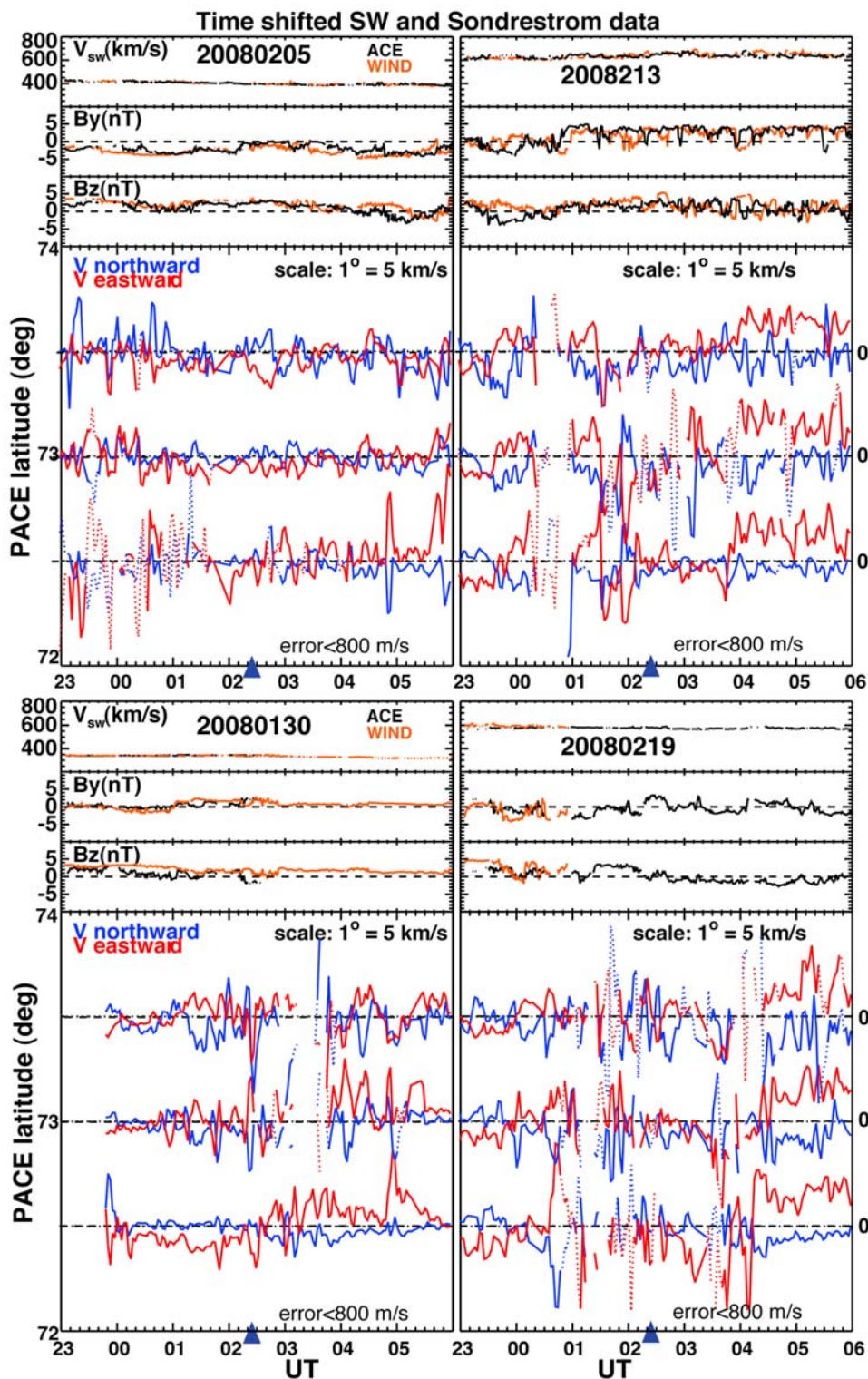


Figure 5. Same as Figure 2, except for four of our nightside Sondrestrom runs. Flows are shown at three latitudes from 72.5° to 73.5° .

[15] We have only one nightside Sondrestrom run so far with prolonged steady southward IMF conditions, which occurred from ~ 2230 to 0215 UT on 4–5 March 2008. Flows from this run are shown in Figure 6 (left). Figure 6 also shows examples with enhanced IMF fluctuations, two during high-speed solar wind streams (1 February and 26 March

2008) and the third during slow-speed solar wind (1 May 2008). Shown most dramatically in Figure 6 is an enhancement in equatorward convection flow during the enhanced IMF fluctuation conditions. Thus for both northward and southward IMF, the Sondrestrom observations show flows that indicate there is enhanced earthward convection within

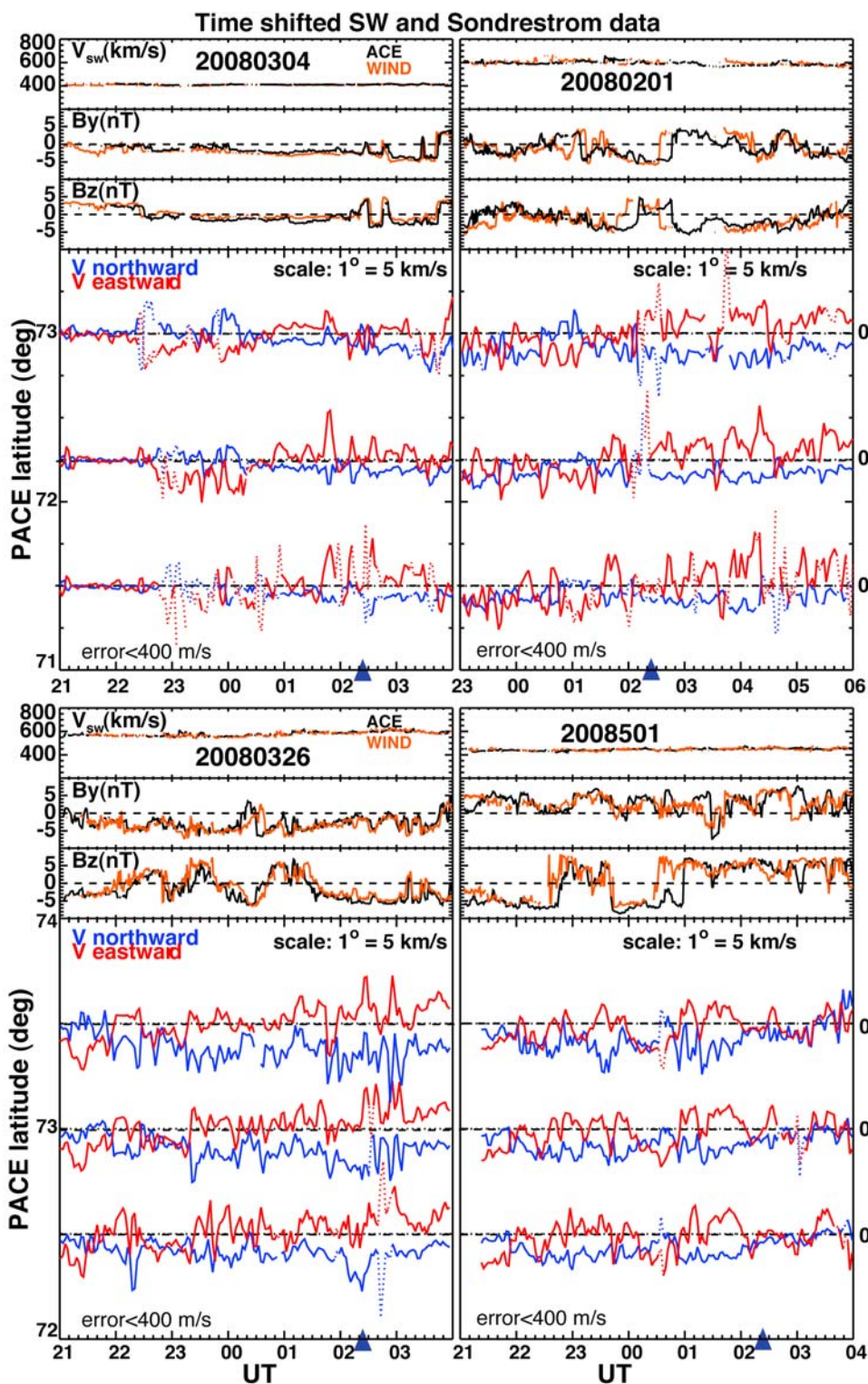


Figure 6. Same as Figure 2, except for four of our nightside Sondrestrom runs. Flows are shown at three latitudes from 72.5° to 73.5° .

the plasma sheet under fluctuating IMF conditions. Together with the PFISR observations discussed with Figure 4, this suggests that earthward convection is enhanced throughout the plasma sheet during fluctuating IMF.

[16] An enhancement in the level of flow fluctuations on the nightside in response to an enhancement in interplanetary

fluctuations was clearest for northward IMF conditions in the line plots for the three sets of radar runs discussed above. To check whether this enhancement also occurs for nonnorthward IMF conditions, we show in Figure 7 the power spectral densities (PSD) of convection flow speeds and of P_{dyn} and IMF B_z for a steady southward IMF run and a fluctuating

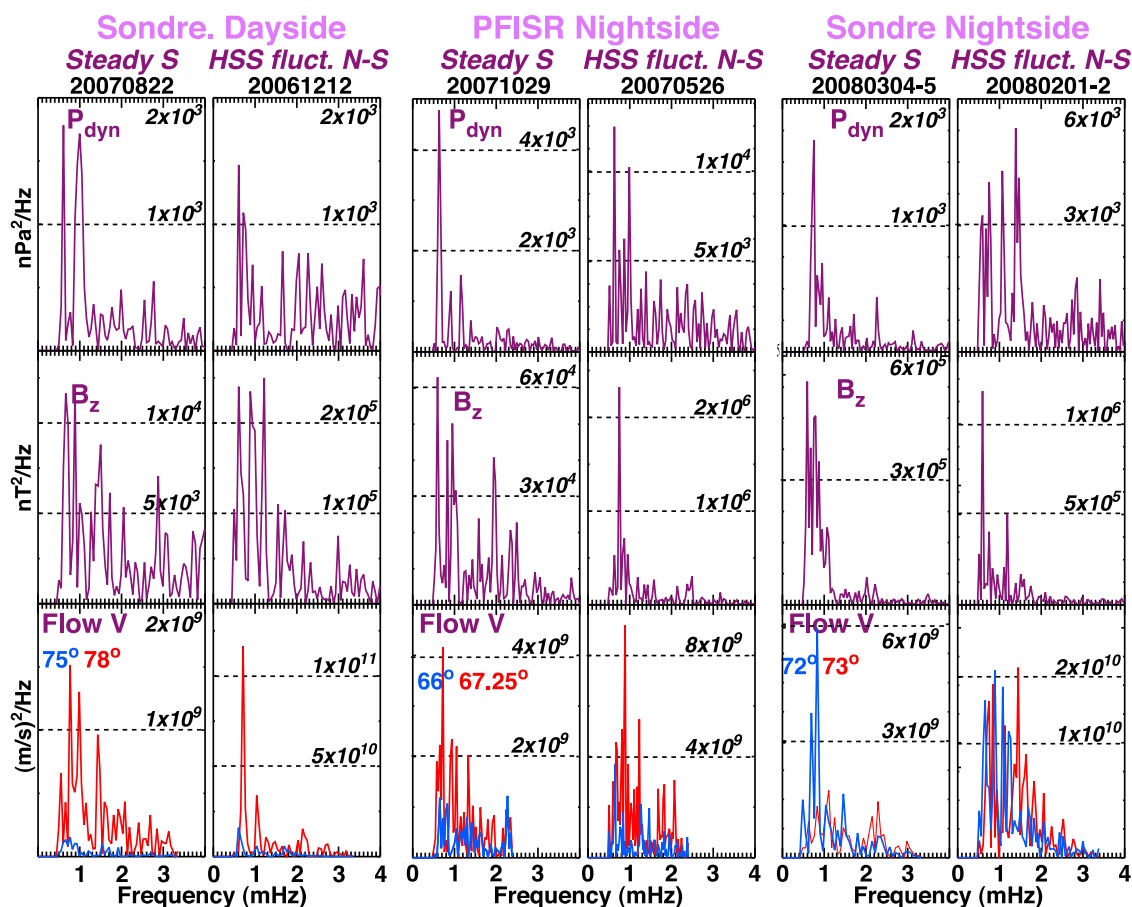


Figure 7. Power spectral densities of convection flow speeds at two invariant latitudes and of P_{dyn} and IMF B_z for a steady southward IMF run and a fluctuating north–south IMF run over the frequency range 0.5–3.4 mHz for each of the three sets of radar runs.

north–south IMF run over the frequency range 0.5–3.4 mHz for each of our radar sets. The PSD show evidence that the results of *Kim et al.* [2009] for the dayside Sondrestrom observations also apply to the nightside plasma sheet. The PSD of the convection flow speeds have large peaks in the range of the lowest ULF Pc5 frequencies (0.7–1.3 mHz), and P_{dyn} and IMF B_z also have large PSD in that frequency range. In addition to this resemblance of the spectral shapes, the PSD of convection flow speeds can be seen to be larger for the fluctuating IMF B_z runs than during the steady southward IMF run. That these trends are seen within the dayside polar cap and throughout the nightside plasma sheet is consistent with the possibility that solar wind fluctuations drive large amplitude oscillations throughout the global convection system.

3.2. THEMIS Observations

[17] We expect that the convection features discussed above that are seen within the ionosphere by the radars should also be seen within the tail plasma sheet, though these effects would be in addition to the plasma sheet flows associated with magnetic field changes, such as substorm dipolarizations, which do not map to the ionosphere. Figures 8 and 9 show the three components of plasma velocity observed by THEMIS spacecraft within the inner plasma sheet during selected orbits. Also shown for each

orbit are the Weimer-mapped solar wind speed, dynamic pressure, and IMF B_y and B_z . Flows are shown only from the three inner THEMIS spacecraft, since the outer two spacecraft were often near the outer boundary of the plasma sheet or within the lobes. THEMIS E closely follows THEMIS D in the same orbit with apogee at a radial distance $r \sim 11 R_E$, and observations are shown for 9 h periods when these two spacecraft were within the vicinity of midnight and mostly at $r \geq 9 R_E$. Flows from the innermost THEMIS A spacecraft are also shown for orbits that reached the nightside plasma sheet, these flows being of interest here when the spacecraft was tailward of about $x = 6.5 R_E$. All velocities and positions are in GSM coordinates. Vertical dotted lines in the velocity panels give the times of give substorm onsets. These onsets were identified by having both the typical magnetic dipolarization signature within the inner plasma sheet (see Figure 10) and an auroral brightening followed by expansion seen by the THEMIS ground all-sky imager array [*Mende et al.*, 2008]. The strength and duration of the ensuing expansion phase were not considered. Onset times were obtained to within ~ 1 – 2 min accuracy using the auroral images, though precise onset timing is not of importance here. Auroral images usable for substorm identification are not available for the second half of the period shown in Figure 9 (left; owing to the MLT of midnight being west of Alaska) and during the entire period of the orbit in Figure 9

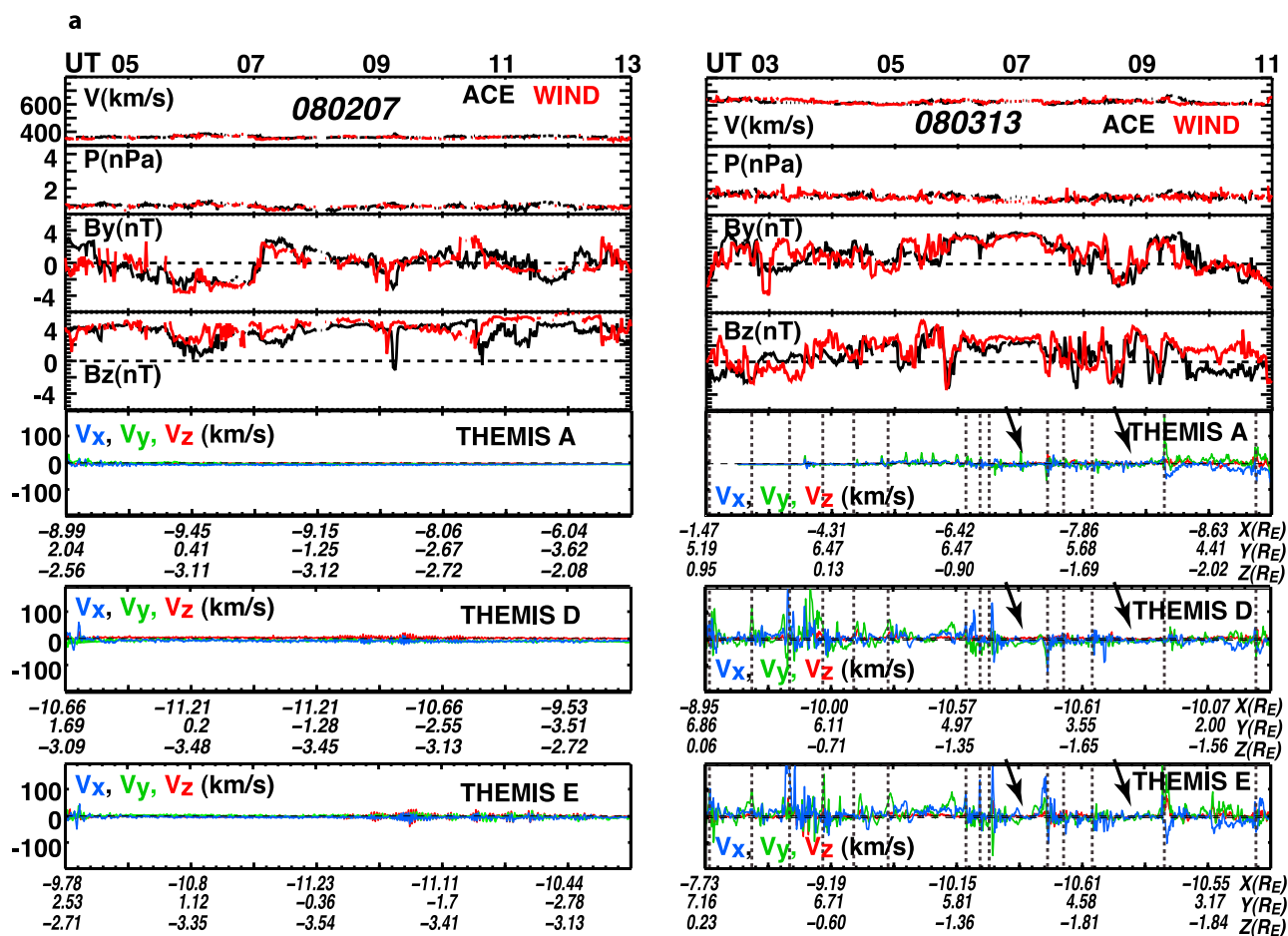


Figure 8. Three components of plasma velocity observed by Time History of Events and Macroscale Interactions during Substorms (THEMIS) spacecraft within the inner plasma sheet during two orbits. Also shown for each orbit are the Weimer-mapped solar wind speed, dynamic pressure, and IMF B_y and B_z . Vertical dotted lines in the velocity panels give the times of substorm onsets identified by having both the typical magnetic dipolarization signature within the inner plasma sheet and an auroral brightening followed by expansion seen by the THEMIS ground all-sky imager array. Arrows identify prolonged periods of flows up to a few tens of kilometers per second between substorm onsets under northward IMF.

(right; owing to moonlight and clouds). Substorms were identified only from the inner plasma sheet dipolarizations for these periods, and such onset identifications are indicated by a lighter dotted line than for the other onsets. Magnetic field dipolarizations are generally associated with energetic particle injections, and *Kim et al.* [2008] found that $\sim 90\%$ or energetic, particle injections at geosynchronous orbit observed during high-speed stream periods are associated with visible auroral onsets. Thus, while our onset identification for the events without images may have some errors, our use of identifiable dipolarizations for these events is sufficient for obtaining a reasonable estimate of the frequency of substorm occurrence for the two examples in Figure 9.

[18] The examples in Figure 8 have been selected to have predominantly steady northward IMF (Figure 8, left) or to have predominantly northward IMF with large amplitude Alfvénic fluctuations (Figure 8, right). No substorms and almost no significant plasma flow were detected during the entire northward IMF period of 2 February 2008 in Figure 8 (left). Also, no substorms and very little significant plasma

flow were identified during the prolonged period of northward IMF from shortly after 0400 to ~ 1040 UT in the 5 February 2008 example. The highly variable flows of magnitude up to ~ 50 km/s observed for ~ 15 min after the substorm onset near 0400 UT on 5 February are typical of what is observed following an substorm onset, and there is a more prolonged period of flows following the onset near 1040 UT when the IMF B_y was at ~ -3 to -4 nT and B_z was small.

[19] The lack of flows and substorm onsets during the above orbits is what is normally expected for northward IMF conditions. However, the flows and substorm occurrence are dramatically different during the orbits with large amplitude Alfvénic fluctuations (Figure 8, right), as was also seen for the flows in the ground radar observations for predominantly northward IMF conditions. The IMF was predominantly northward from ~ 0330 to 0930 UT in the 13 March 2008 example and for all but from ~ 0300 to 0340 and from 0510 to 0620 UT in the 12 February 2008 example. But despite this predominantly northward IMF, substorms onsets were observed on the average more than once per hour! These

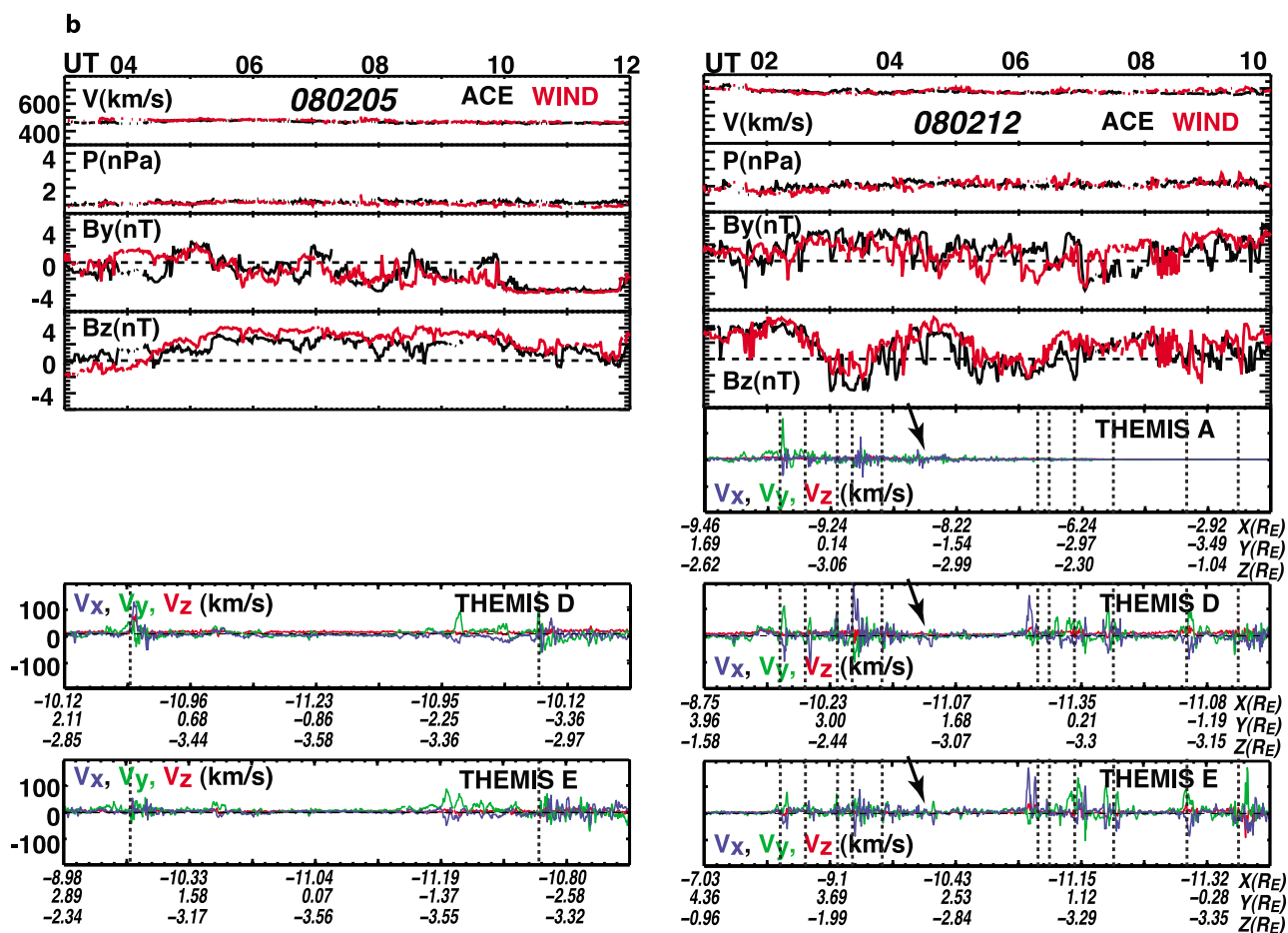


Figure 8. (continued)

onsets were followed by typical substorm-related flow bursts. However, in addition to these flows, there were flows up to a few tens of kilometers per second between the substorm onsets during prolonged periods of northward IMF, such as from ~0500 to 0600 UT and from ~0815 to 0915 UT on 13 March and from ~0400 to 0500 UT on 12 February (indicated by arrows in Figure 8). In Figure 9, the 21 February 2008 orbit (Figure 9, left) includes a prolonged period of relatively steady southward IMF from ~0930 to 1600 UT. On 19 February 2008 (Figure 9, right), there was highly fluctuating IMF with much southward IMF before 0810 UT and mostly northward IMF from ~0900 to 1130 UT. It can be seen that neither the flows nor the substorms occurrence are larger or more frequent during the steady southward IMF orbit than for the fluctuating IMF orbit in Figure 9 or the fluctuating IMF orbits in Figure 8.

[20] The THEMIS observations in Figures 8 and 9 indicate that, consistent with the radar observations, fluctuating IMF conditions lead to substantial plasma sheet flows even for northward IMF. While not clear from the THEMIS observations, the radar observations suggest that these flows should enhance the earthward convection and thus the earthward penetration of the plasma sheet. This should enhance plasma pressures within the inner plasma sheet. That there is frequent substorm occurrence in the examples shown above under fluctuating northward IMF conditions is consistent with

this possibility. As a test of whether this occurs, Figure 10 compares the plasma sheet pressures during the 7 February 2008 orbit with steady northward IMF and the 12 February 2008 orbit with predominant northward and fluctuating IMF. These two examples were chosen because the THEMIS A, D, and E spacecraft were all at approximately the same radial distances in the vicinity of midnight on both orbits, and, in addition, THEMIS B on 7 February and THEMIS C on 12 February were further from Earth and at similar radial distances. Shown in Figure 10 is the thermal plasma pressure P_{th} and the total plasma pressure at the center of the plasma sheet ($P_{tot} = P_{th} + B_x^2 + B_y^2$) as estimated from the tail pressure balance assumption [Xing *et al.*, 2009]. Note that, while THEMIS B was mostly within the lobes on 7 February and THEMIS C was well away from the center of plasma sheet, P_{tot} gives a meaningful pressure comparison. The magnetic field measured on each spacecraft is also shown in Figure 10, and the substorm onsets are indicated by vertical dotted lines.

[21] Figure 10 shows a greatly enhanced variability of the pressures during the fluctuating IMF orbit than during the steady IMF orbit, much of the variation being associated with the substorm related stretching and dipolarization of the magnetic field. However, the pressures during the steady northward IMF orbit (7 February) vary very smoothly. To facilitate comparison of the values of P_{tot} between the two orbits, a thin horizontal dotted line is drawn in each pressure

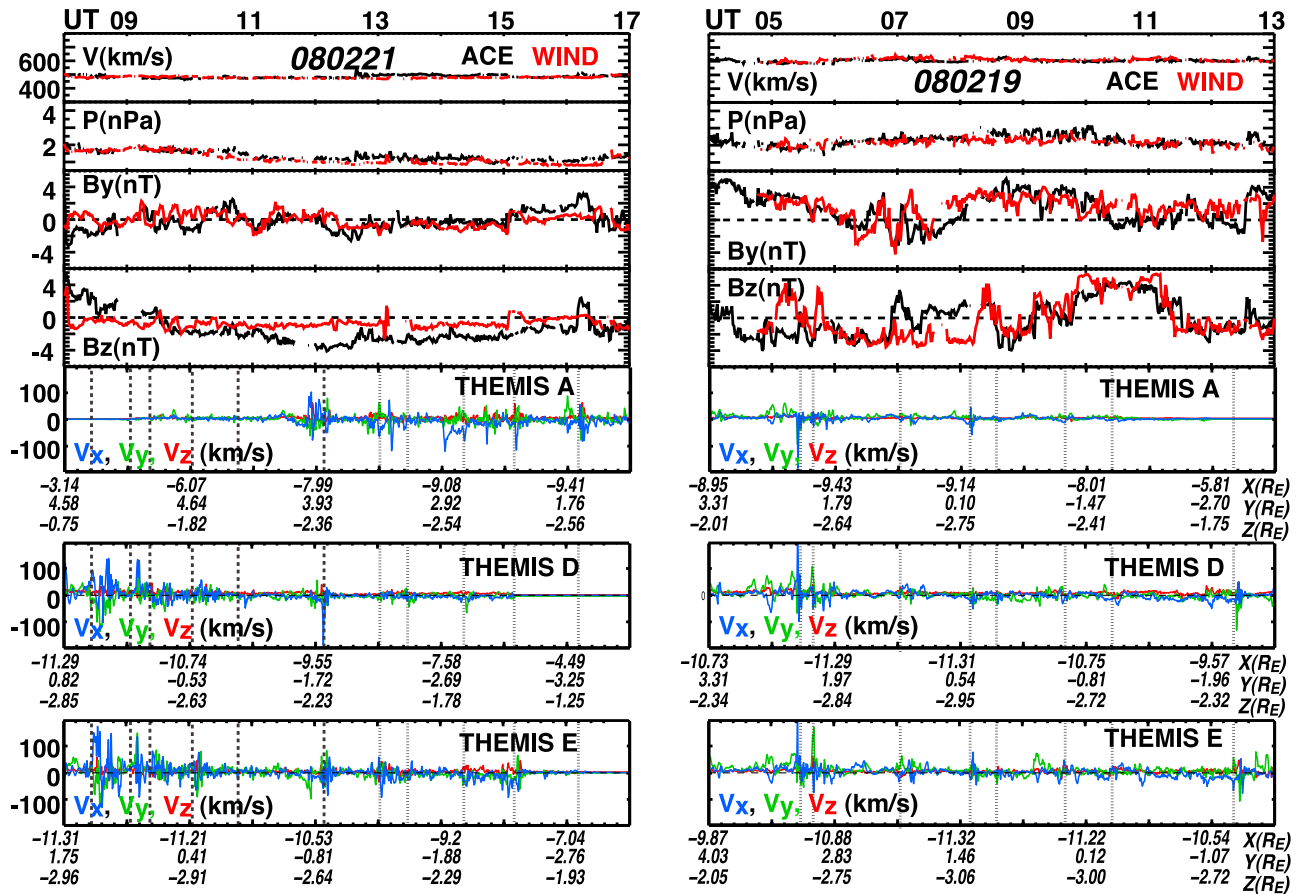


Figure 9. Same as Figure 8, except that light vertical dotted lines give the times of substorm onsets identified only by their magnetic dipolarization signature since usable all-sky image data are not available.

panel at the minimum value of P_{tot} observed during the 7 February orbit of the corresponding spacecraft. It can clearly be seen that the pressures on 12 February at THEMIS D and E remained above the minimum values seen on 7 February throughout the entire period shown. The higher pressure of 12 February can also be seen by comparing values of P_{tot} at similar x distances. The observed pressure difference further out in the plasma sheet is much larger, P_{tot} on THEMIS C on 12 February being over a factor of two larger than P_{tot} on THEMIS B on 7 February over almost the entire portions of the orbits shown. THEMIS A covered about the same radial position range between 0800 and 1000 UT on 7 February as it did between 0330 and 0530 UT on 12 February, and it can be seen that P_{tot} in this region was larger on 12 February than on 7 February. While a far more thorough study of pressures in this region is needed, these comparisons for one pair of orbits shows higher pressure throughout the radial distance range of $\sim 8-19 R_E$ during the orbit with fluctuating northward IMF conditions than during the orbit with steady northward IMF. This is as expected from earthward convection being enhanced under fluctuating IMF conditions.

4. Conclusions

[22] We have examined PFISR and Sondrestrom ISR observation of flows within the ionospheric mapping of the

nightside plasma sheet and THEMIS spacecraft observations within the nightside plasma sheet to investigate whether the features found by *Kim et al.* [2009] within the dayside polar cap are also seen within the nightside plasma sheet. We find evidence that this is indeed the case, ULF fluctuations of the IMF substantially enhancing convection and the IMF fluctuations being reflected in the nightside convection flows.

[23] In addition, the flow observations show evidence that interplanetary ULF fluctuations give an enhancement of earthward convection within the plasma sheet, which could be associated with a reduction in shielding. This would be expected to increase plasma pressures within the inner plasma sheet. We found evidence for such a pressure increase over the radial distance range of $\sim 8-19 R_E$ by making pressure comparisons with four THEMIS spacecraft between an orbit under steady northward IMF conditions and an orbit under predominant northward, but strongly fluctuating, IMF conditions. We also found evidence that the enhancement in convection and plasma sheet pressures within the inner plasma sheet may lead to a dramatic increase in substorm occurrence under northward IMF conditions.

[24] The comparisons in this paper thus give evidence that solar wind ULF fluctuations have a substantial effect on global convection, and are consistent with the possibility that long-period ULF oscillations can be an important contributor to the large-scale transfer of solar wind energy to the

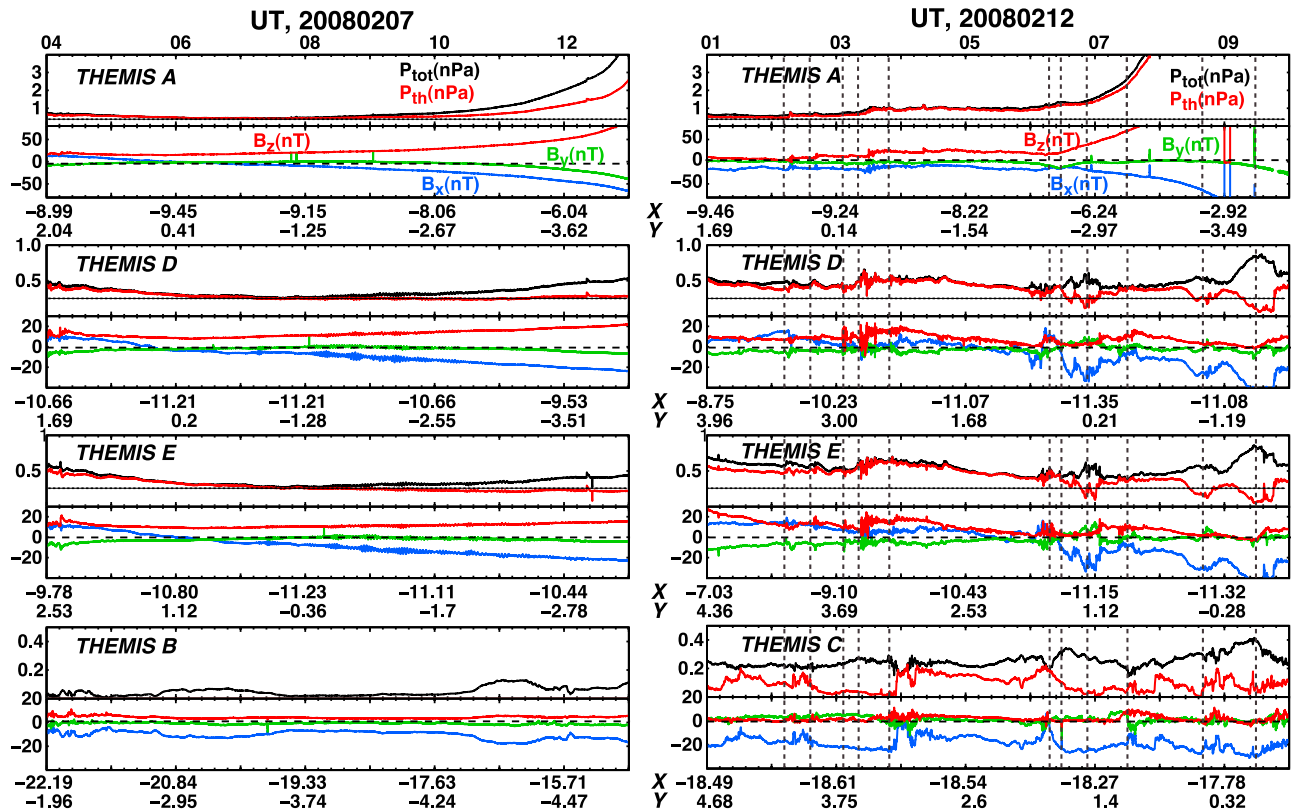


Figure 10. Thermal plasma pressure P_{th} and the estimated total pressure at the center of the plasma sheet $P_{tot} (= P_{th} + B_x^2 + B_y^2)$. The magnetic field measured on each spacecraft is also shown, and substorm onsets are indicated by vertical dotted lines.

magnetosphere-ionosphere system, to plasma sheet structure and dynamics, and to the occurrence of substorms.

[25] However, it must be remembered that the results of Kim *et al.* [2009] within the dayside polar cap were substantiated with detailed statistical analysis, while the results in this paper must be regarded as preliminary since they were obtained only from comparison between the most ideal examples that are currently available. More data is being accumulated both with the radars and with THEMIS, so that far more detailed testing of our results should be possible in the future. It should also be interesting to use the more global observations from the Super Dual Auroral Radar Network (SuperDARN) and PolarDARN radars, as well as from the new Resolute Bay ISR within the polar cap. Additionally, it would be interesting to determine how substorms under northward, but fluctuating, IMF conditions compare to substorms under southward IMF conditions.

[26] **Acknowledgments.** Work at UCLA and Berkeley was supported by the U.S. National Science Foundation grants ATM-0639312 and ATM-0646233 and NASA contract NAS5-02099. The Sondrestrom ISR and PFISR measurements and analysis are supported under Cooperative agreement ATM-0608577 between the U.S. National Science Foundation and SRI International. The FGM team under the lead of the Technical University of Braunschweig is financially supported through the German Ministry for Economy and Technology and the German Center for Aviation and Space under contract 50 OC 0302. The time-shifted IMF and solar wind data measured by ACE and Wind spacecrafts were obtained from the GSFC/SPDF OMNIWeb interface at <http://omniweb.gsfc.nasa.gov>. We thank M. Kessel and J. Bortnik for their assistance in the spectral analysis of solar wind and radar data.

[27] Amitava Bhattacharjee thanks Dong-Hun Lee and another reviewer for their assistance in evaluating this paper.

References

- Angelopoulos, V. (2008), The THEMIS Mission, *Space Sci. Rev.*, *141*, 5–34, doi:10.1007/s11214-008-9336-1.
- Auster, H. U., et al. (2008), The THEMIS fluxgate magnetometer, *Space Sci. Rev.*, *141*, 235–264, doi:10.1007/s11214-008-9365-9.
- Boudouridis, A., L. R. Lyons, E. Zesta, and J. M. Ruohoniemi (2007), Dayside reconnection enhancement resulting from a solar wind dynamic pressure increase, *J. Geophys. Res.*, *112*, A06201, doi:10.1029/2006JA012141.
- de la Beaujardière, O., L. R. Lyons, J. M. Ruohoniemi, E. Friis-Christensen, C. Danielsen, F. J. Rich, and P. T. Newell (1994), Quiet-time intensifications along the poleward auroral boundary near midnight, *J. Geophys. Res.*, *99*, 287–298.
- Kim, H.-J., D.-Y. Lee, and L. R. Lyons (2008), Are repetitive particle injections during high-speed solar wind streams classic substorms?, *J. Geophys. Res.*, *113*, A08205, doi:10.1029/2007JA012847.
- Kim, H.-J., L. R. Lyons, S. Zou, A. Boudouridis, D.-Y. Lee, C. Heinselman, and M. McCready (2009), Evidence that solar wind fluctuations substantially affect the strength of dayside ionospheric convection, *J. Geophys. Res.*, *114*, A11305, doi:10.1029/2009JA014280.
- Lyons, L. R., T. Nagai, G. T. Blanchard, J. C. Samson, T. Yamamoto, T. Mukai, A. Nishida, and S. Kokubun (1999), Association between Geotail plasma flows and auroral poleward boundary intensifications observed by CANOPUS photometers, *J. Geophys. Res.*, *104*, 4485–4500.
- Lyons, L. R., S. Zou, C. J. Heinselman, M. J. Nicolls, and P. C. Anderson (2009), Poker Flat radar observations of the magnetosphere-ionosphere coupling electrodynamic of the Earthward penetrating plasma sheet following convection enhancements, *J. Atmos. Terr. Phys.*, *71*, 717–728, doi:10.1016/j.jastp.2008.09.025.
- McFadden, J. P., C. W. Carlson, D. Larson, V. Angelopoulos, M. Ludlam, R. Abiad, B. Elliott, P. Turin, and M. Marckwordt (2008), The THEMIS ESA plasma instrument and in-flight calibration, *Space Sci. Rev.*, *141*, 277–302, doi:10.1007/s11214-008-9440-2.

- Mende, S. B., S. E. Harris, H. U. Frey, V. Angelopoulos, C. T. Russell, E. Donovan, B. Jackel, M. Greffen, and L. M. Peticolas (2008), The THEMIS array of ground-based observatories for the study of auroral substorms, *Space Sci. Rev.*, *141*, 357–387, doi:10.1007/s11214-008-9380-x.
- Weimer, D. R., D. Ober, N. C. Maynard, W. J. Burke, M. R. Collier, D. J. McComas, N. F. Ness, and C. W. Smith (2002), Variable time delays in the propagation of the interplanetary magnetic field, *J. Geophys. Res.*, *107*(A8), 1210, doi:10.1029/2001JA009102.
- Xing, X., L. R. Lyons, V. Angelopoulos, D. Larson, J. McFadden, C. Carlson, A. Runov, and U. Auster (2009), Azimuthal plasma pressure gradient in quiet time plasma sheet, *Geophys. Res. Lett.*, *36*, L14105, doi:10.1029/2009GL038881.
- Zesta, E., L. R. Lyons, and E. Donovan (2000), The auroral signature of earthward flow bursts observed in the magnetotail, *Geophys. Res. Lett.*, *27*, 3241–3244.
- Zesta, E., L. Lyons, C.-P. Wang, E. Donovan, H. Frey, and T. Nagai (2006), Auroral poleward boundary intensifications (PBIs): Their two-dimensional structure and associated dynamics in the plasma sheet, *J. Geophys. Res.*, *111*, A05201, doi:10.1029/2004JA010640.
- Zou, S., L. R. Lyons, M. A. McCready, and C. J. Heinselman (2008), High-time resolution dayside convection monitoring by incoherent scatter radar and a sample application, *J. Geophys. Res.*, *113*, A01203, doi:10.1029/2007JA012364.
- Zou, S., L. R. Lyons, M. J. Nicolls, and C. J. Heinselman (2009), PFISR observations of strong azimuthal flow bursts in the ionosphere and their relation to nightside aurora, *J. Atmos. Terr. Phys.*, *71*, 729–737, doi:10.1016/j.jastp.2008.06.015.
-
- V. Angelopoulos, Department of Earth and Space Sciences, Institute for Geophysics and Planetary Physics, University of California, 405 Hilgard Ave., Los Angeles, CA 90095-1567, USA.
- K.-H. Fornacon, Institut für Geophysik und Extraterrestrische Physik, Technische Universität Braunschweig, Mendelssohnstrasse 3, D-38106 Braunschweig, Germany.
- C. Heinselman and M. J. Nicolls, Center for Geospace Studies, SRI International, 333 Ravenswood Ave., Menlo Park, CA 94025, USA.
- H.-J. Kim, L. R. Lyons, X. Xing, and S. Zou, Department of Atmospheric and Oceanic Sciences, University of California, 405 Hilgard Ave., Los Angeles, CA 90095-1565, USA. (larry@atmos.ucla.edu)
- D. Larson, J. McFadden, and A. Runov, Space Sciences Laboratory, University of California, 7 Gauss Way, Berkeley, CA 94720, USA.
- D.-Y. Lee, Department of Astronomy and Space Science, Chungbuk National University, 410 Sungbong-Ro, Heungduk-Gu, Cheongju, Chungbuk 361-763, South Korea.